SPRI Time- and Position-Tagged Radio Echo Profiles for Canadian Arctic (CA), 2000, with derived and ancillary data

This data set contains radar sounder profiles from the SPRI 100 MHz ice-penetrating radar instrument over Devon and Ellesmere islands in the Canadian Arctic (CA). Along with the radar profile data, the archive includes derived and ancillary data, plus software code produced for acquisition and working up of data. The data were collected under funding from a UK Natural Environment Research Council (NERC) grant (GR3/12469) to Prof. J. A. Dowdeswell.

In April 2000, staff from Scott Polar Research Institute (SPRI)[1], University of Cambridge undertook airborne Radio Echo Sounding (RES) surveys of the Devon Ice Cap on Devon Island, and the outlet glaciers of Agassiz and Prince of Wales ice caps on Ellesmere Island, Arctic Canada. Participants were J. A. Dowdeswell, T. J. Benham, M. R. Gorman, R. P. Bassford and M. Sharp (University of Alberta). A grid pattern was flown over the Devon Ice Cap, with the intention of deriving Digital Elevation Models (DEMs) of the ice cap and its ice thickness, whilst, on Ellesmere Island, the focus was on the approximate centre-line of outlet glaciers, with some across profiles also flown. The instrument platform was a Kenn Borek Aviation DHC-6 Twin Otter aircraft (C-GKBC), with two half-wave dipole antennae mounted, one beneath each of the aircraft wings (one for transmitting and the second for receiving). Antenna gain was 8 dB (one-way).

Geographical Coverage

[1] Based at that time in Bristol Glaciology Centre

Overview

Parameter(s):	• Sensor Characteristics > Amplitude • Radar > Return Power • Derived > Ice Thickness
Spatial Coverage:	• N: 81° 0' 32" N • S: 74° 27' 57" N • E: 71° 48' 1" W • W: 94° 59' 18" W
Spatial Resolution:	• Varies x Varies
Temporal Coverage:	• 4th – 15th April 2000
Data Format(s):	• NetCDF • SPRI bespoke Binary data
Platform(s)	DeHavilland DHC-6 Twin Otter C-GKBC
Sensor(s):	SPRI 100 MHz
Version:	V1
Data Contributor(s):	Julian Dowdeswell, Toby Benham, Michael Gorman, Robin Bassford, Martin Sharp. Collated for archival by Toby Benham and archived by Frazer Christie (SPRI).

Data Citation

As a condition of using these data, you must cite the use of this data set using the following citation:

Dowdeswell, J. A., Benham, T. J., Gorman, M. R., Burgess, D., & Sharp, M. J. (2004). Form and flow of the Devon Island Ice Cap, Canadian Arctic. Journal of Geophysical Research - Earth Surface, 109(F2). doi:10.1029/2003JF000095

Dowdeswell, J.A., Benham, T.J., Gorman, M., Bassford, R., & Sharp, M. (2021). Scott Polar Research Institute Arctic Airborne Radio-Echo Sounding Datasets: Canadian Arctic 2000. https://doi.org/10.17863/CAM.69708.

Archive Structure

Table 1 outlines the main directories for this archive and the content within.

Table 1: Canadian Arctic RES 2000 - structure of archive

Directory	Description
RES2000	Radio Echo Sounding and Ancillary data from 2000 Survey of Canadian Arctic

Scott Polar Research Institute

Directory	Description
RES2000/ArchiveGeneral	Information and software utilities+scripts used to produce the NetCDF content within this archive.
RES2000/DerivedProducts	Spatial data products (grid, point) produced from SPRI RES 2000 data. Ice thicknesses, Surface and Bed Elevations.
RES2000/DerivedProducts/CD	Content of CD of derived products (grids, point measurements, etc.) for Devon Ice Cap (DIC) created from 2000 RES survey and issued in 2002 to a small number of persons. See file README.txt, which further explains the CD content.
RES2000/DerivedProducts/CD/DEMs	Contains gridded and vector data relating to DIC RES-derived DEMs. Grids are given in UTM17N WGS84; vector data is given in the same UTM projection, as well as in geographic (WGS84) co-ordinates. Some files are given relating to organization of the data within a Project to be read with the (now defunct) ESRI ArcView GIS software.
RES2000/DerivedProducts/CD/DEMs/Grids	ESRI ArcInfo GRID format data for DIC DEMs. See elsewhere in Archive if this format cannot be read or translated.
RES2000/DerivedProducts/CD/DEMs/latlong	ESRI Shapefiles in Geographic co-ordinates (WGS84) for DEMs and input / ancillary data coverages.
RES2000/DerivedProducts/CD/DEMs/Legends	ESRI ArcView Legend files for display of coverage data.
RES2000/DerivedProducts/CD/DEMs/UTM17N	ESRI Shapefiles projected into UTM17N co-ordinates (WGS84) for DEMs and input / ancillary data coverages.
RES2000/DerivedProducts/CD/Hypso	Contains a number of Excel spreadsheets giving Hypsometric calculations relating to the DEM grids.
RES2000/DerivedProducts/CD/Overview	Overview of DEMs contained on the CD. Document DEMstats.doc gives statistics and hypsometric graphs.
RES2000/DerivedProducts/CD/Production	Metadata relating to Production of RES-derived data. Document DEMinterpolation.doc gives details of the process used to generate Gridded data, and gives an Error Budget calculation. Document DEMmetadata.doc gives metadata for (Shapefile) Coverages and Gridded data contained in the CD folders.
RES2000/RES	Radio Echo Sounding Raw and Ancillary data.
RES2000/RES/RAW	Radio Echo Sounding Raw and Ancillary data. 'Raw' refers generally to the fundamental Binary dataset collated from raw measurement files (although some raw GPS datafiles are included) - e.g. RES waveform data acquisitions are stored in .DTA files, tagged with positional data.
RES2000/RES/RAW/GPS_SSF	Trimble GPS data for Base Stations (Resolute, Eureka), Rover (i.e. Twin Otter survey aircraft), and Differential Correction processing of these to remove Selective Availability induced error.
RES2000/RES/RAW/RESdata	SPRI Bespoke format data files for Radar (.DTA), Position (.GPS, from serial link), Pressure Analogue-Digital (.PAD - single capture; .PMN - averaged), and interface (surface, bed) tracking results (.TRK). Files are named 'XXXXXXXXX.xtn', where 'XXXXXXXXX' is the Flightline ID, and .xtn the file extension relevant to the data type, e.g. 987123456.DTA. Assorted related files are given in subdirectories relating to Concatenation of original acquisition files, Calibration, text Extractions from raw data, and images printed from profile displays.
RES2000/RES/RAW/RESdata/Calibration	Various files relating to Calibration of: Radar data DNs to dB; Radar spreading loss and attenuation in air; aircraft flying height from PAD vs GPS/over-sea Terrain Clearance; GPS unit time vs acquisition PC time.
RES2000/RES/RAW/RESdata/Extractions	Various files created by extraction of profile data from our software to a tab/comma-delimited text format

Directory	Description
RES2000/RES/RAW/RESdata/FileCatenation	Various files relating to the concatenation of acquisition data files into complete Flightline data records.
RES2000/RES/RAW/RESdata/ProfileImages	Various images of glacier/ice cap RES profiles printed from our software to aid manual analysis and checking.
RES2000/RES/RAW/RESdb	Database files (.DBF records; .MDX indexes) used by our RES Software, including Interpolation utility for Devon Ice Cap grid production. Includes some database files used in Pressure-Height calibration and Cross Points Analysis.
RES2000/RES/RAW/RESimages	Plan view imagery (Landsat) used to orient RES profile analysis within our Tracker software. Subdirectory holds images output from Tracker with base location image overlain with interface track marks, etc.
RES2000/RES/RAW/RESimages/ImgsOutput2000	Images output from Tracker with base location image overlain with interface track marks, etc.
RES2000/RES/Software	This directory contains items of (C/C++) code by T Benham, produced for and used during the acquisition and working up of Canadian Arctic 2000 RES survey data. Code was produced using Borland C++ Builder v4 (now superceded by Embarcadero). The (.h) header files within the code act as a definition of binary file data structures.
RES2000/RES/Software/Acquisition v1.03	This is the data acquisition software used on the ARCOM industrial rackmount PC during survey flying. Data was acquired in a series of ~10MB files, to be stitched together into single files for each Flightline (in order to be able to fit data onto ZIP disks for transfer from the aircraft).
RES2000/RES/Software/general	A set of general utility programs developed. These are DBmainttools (database maintenance), PH_Editor (Pressure-Height data handling), SSFreadProject (Trimble GPS SSF file content reading), mapcontour (for height extraction from raster contour map). These may be at various stages of maturity / functionality and are mostly experimental.
RES2000/RES/Software/reduction	Programs created during the data processing of the RES and other data acquired. As for 'general' category, some of these may be at various stages of maturity / functionality (excepting tracker utility) and some may be experimental.
RES2000/RES/Software/reduction/crosspts	for Crossing Point Analysis of surface/bed elevations and ice thicknesses
RES2000/RES/Software/reduction/Drutilities	general data reduction utilities
RES2000/RES/Software/reduction/extractor	for extraction of data points (experimental?)
RES2000/RES/Software/reduction/interpolation	Utilities for data grid Interpolation (and its Setup)
RES2000/RES/Software/reduction/migration	for 2D migration of profile data (experimental - not used in final data extraction)
RES2000/RES/Software/reduction/navigation	for processing of positioning data, and its refinement
RES2000/RES/Software/reduction/tracker	for display of RES profile data (including tagged positions, etc.) and interface tracking.

Detailed Data Description

Radar Data

Data Format

The data files are given in two formats:

- Bespoke binary data files (.DTA and .TRK) as used for original data analysis
- NetCDF (.nc) format, for compatibility with other public RES data sources.

SPRI Bespoke Binary files

Survey flights were divided into a number of separate data-gathering legs, each identified by a (nine-digit) numeric ID, calculated at time of file creation as the number of seconds since a reference date of 1st January 1970 (minus a local-time offset of 4 hours vs GMT). This allowed automatic generation of a flight leg ID which would never clash with other filenames, and be relatable to time of data acquisition.

For example, file **954877643.DTA** represents a data leg commencing at 15:47:23 (local time) on the 4th April 2000. Note that, during acquisition, data files were split into size-limited segments, so as to enable transfer from the aircraft by Zip disk. These were combined at the start of data analysis, merging in Pressure - .PAD – file and GPS data on a timestamp basis, with the final file named according to the first merged segment. The pre-merge data files are not retained within this archive.

During analysis of the RES data, surface and bedrock interfaces were picked against displays of RES waveform data, and the resulting pick locations stored in binary .TRK files.

SPRI Binary .DTA files

The content of .DTA files is as follows:

RES_Data_Header
RESsounding
RESsounding
.
.
.
RESsounding

where *RES_Data_Header* occupies the same space as subsequent *RESsounding* records (i.e. record 0), and holds information about the file content, used in display and processing of the RES data. The data and header record structures are as defined below in Table 2, and are given in terms of C/C++ code.

Table 2: SPRI RES Binary Data file Record format. Header Record (0) highlighted in blue; Data record in gold; general structure in green.

Record/field structure	Data storage type	Field names
struct RES_Data_Header	struct GBL_datetime	date_time_start;
	struct GBL_datetime	date_time_end;
	float	latitude_from;
	float	longitude_from;
	float	latitude_to;

Record/field structure	**Data storage type**	**Field names**
	float	longitude_to;
	bool	PAD_tagged;
	bool	GPS_tagged;
	float	max_height;
	float	min_height;
	bool	GPS_differentially_corrected;
	bool	PAD_calibrated;
	float	PAD_volt_to_height; // Flightline start value
	float	PAD_convert_drift; // diff bet. start, end
	bool	GPS_calibrated;
	float	GPS_ms_offset; // Flightline start value
	float	GPS_ms_drift; // diff between start and end
	unsigned int	N_waveforms;
	double	image_TL_X; // Bounding UTM
	double	image_TL_Y; // co-ordinates of
	double	image_BR_X; //associated image segment
	double	image_BR_Y; // <FL id>.bmp
	bool	image_registered;
	char	image_name[440];
	RES_filetype	filetype;
	RES_filefmt	filefmt;
	int	samples_per_waveform;
	RES_sampletype	sample_type;
	RES_wavetype	waveform_type;
	unsigned long	timestamp_offset;
RES_filetype[2]	RES_filetype	{**rf_spri**=0, rf_NC, rf_NC_OIB, rf_NC_SPRI, rf_Unknown, rf_Nrf};
RES_filefmt	enum RES_filefmt	{**ff_SPRIbinary**=0, ff_NC, ff_Nff};
RES_sampletype	enum RES_sampletype	{**rs_8bit**=0, rs_float32, rs_Unknown, rs_NStypes};
RES_wavetype	enum RES_wavetype	{**rw_startrise**=0, rw_maxpoint, rw_Nwvtypes};

[2] Enumeration types are defined to allow software operation with other RES data formats, including UTIG, OIB, CReSIS. SPRI data enumeration settings are given in **bold**.

Record/field structure	**Data storage type**	**Field names**
struct RESsounding	char	startacquisitionmark[4]; // ("ZCZC")
	struct RESheader	header;
	unsigned char	datapoint[512]; // Waveform samples
	unsigned char	CRC; // Checksum
struct RESheader	struct GBL_datetime	date_time;
	struct GBL_timestamp	time_sample_timestamp;
	float	GPS_decimal_latitude;
	float	GPS_decimal_longitude;
	float	GPS_elevation; // HAE W84
	float	metres_X; // projected position X
	float	metres_Y; // projected position Y
	float	HAMSL_HAE_offset;// HAMSL=HAE-Offset
	float	Vprecision;
	float	PAD_elevation; // HAE W84
	float	PAD_volt; // holds integer value
	bool	PAD_interpolated_value;
	unsigned char	GPS_source; // 1=Thule; 2=Res/Eureks; 10=Raw
struct GBL_datetime	unsigned char	day_DD;
	unsigned char	month_MM;
	short int	year_YYYY;
	unsigned char	time_HH;
	unsigned char	time_MI;
	unsigned char	time_SS;
	short int	time_MS;
struct GBL_timestamp	long	time;
	short	millitm;
	short	_timezone;
	short	dstflag;
	short	ftime_offset; // diff in ms from 'ftime' result

Table 2: SPRI RES Binary Data file Record format. Header Record (0) highlighted in blue; Data record in gold; general structure in green.

SPRI Binary .TRK files

Scott Polar Research Institute

Track (.TRK) files hold information about surface and bed interfaces picked against display of RES waveform data in A-plot or Z-scope mode within SPRI RES analysis software. The A-plot (or A-scope) display shows a single digitized waveform, with the X-axis steps representing consecutive (50 ns) waveform sampling intervals, and the Y-axis representing the received power, as represented by digitizer data number (DN) values (see Figure 2). The Z-scope display shows a number of consecutive digitized waveforms, with the X-axis representing distance along flight track (in terms of waveform acquisitions or, when related to scale bar, distance travelled), and the Y-axis, the sampling time (50 ns) intervals for each waveform acquisition, starting from transmit time (Tx0) from the aircraft at the top. The greyscale pixel values have brightness determined from waveform sample DN values. Our software also allowed for differentiated data view (instead of raw brightness, the brightness with respect to the average of a neighbouring window of samples), and start-of-rise points view (see Figure 1).

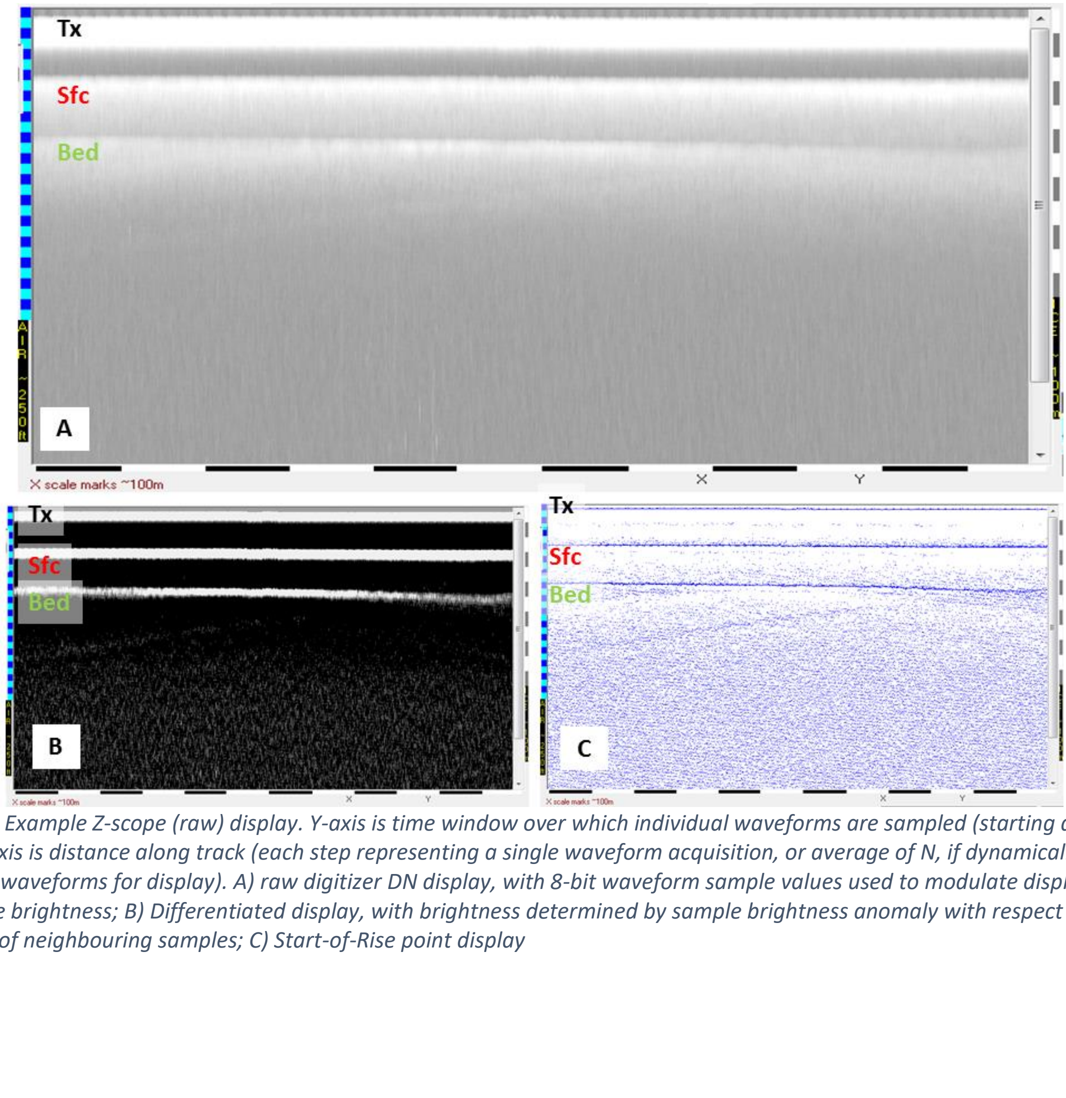

Figure 1: Example Z-scope (raw) display. Y-axis is time window over which individual waveforms are sampled (starting at top); X-axis is distance along track (each step representing a single waveform acquisition, or average of N, if dynamically stacking waveforms for display). A) raw digitizer DN display, with 8-bit waveform sample values used to modulate display greyscale brightness; B) Differentiated display, with brightness determined by sample brightness anomaly with respect to average of neighbouring samples; C) Start-of-Rise point display

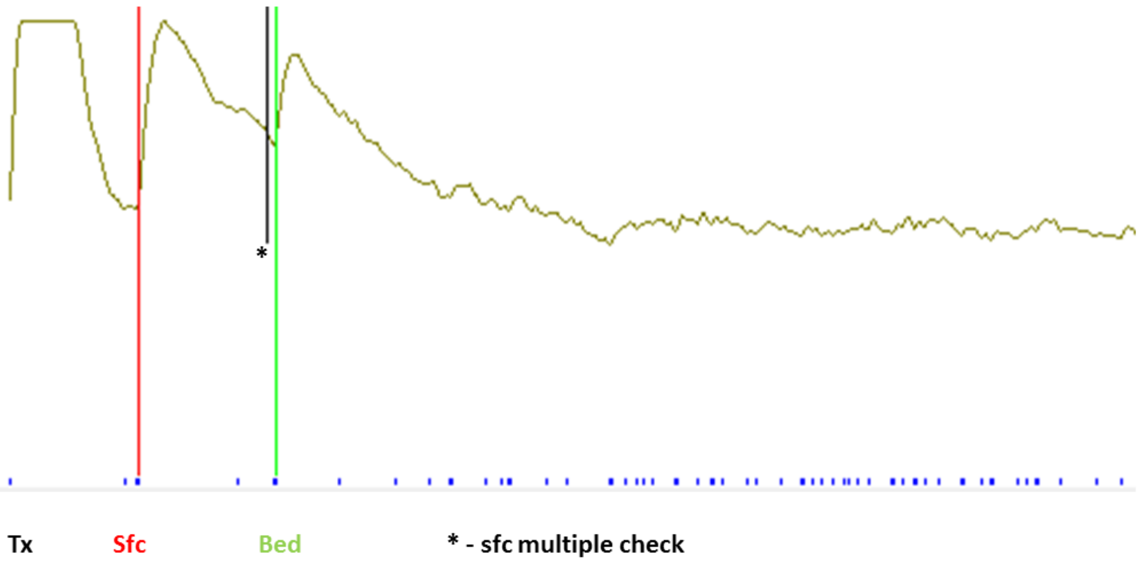

*Figure 2: Example A-scope display, showing a single waveform acquisition. The Y-axis gives the strength of energy received (note saturation of receiver by direct airpath receipt of Tx signal), as a digitizer data number (DN) value; X-axis gives the increasing sampling time, with each step a discrete sampling of the energy received at that number of (50 ns) slots. Blue bars at the bottom mark locations of start-of-rise of power level within the sampled waveform – i.e., the points at which a sustained rise in power level begins. Interface tracking was (optionally) 'snapped' to these marks. Note that interface tracking picks the *start* of a prolonged rise in received power, rather than the peak picking points used for chirped radar data such as that acquired by UTIG HICARS.*

A number of fields were allowed for, several of which were not ultimately used (or were used experimentally for different purposes). As well as principal surface and bed picks, the format allows for alternate surface and bed picks. The latter were used during processing for a number of purposes, including making speculative picks and checking these for alignment with surface imagery features, such as valley walls, foliation, melt ponds and crevassing (Benham and Dowdeswell, 2003). We also defined storage for migrated surface and bed picks, although these were not ultimately used, other than in an experimental fashion. Table 3 shows record structure definitions for .TRK file data, with unused fields marked in red highlight. Clearly there is an amount of 'wasted' space in the archived TRK data, although this equates to a relatively small proportion of the overall dataset, and allows for further analysis starting from the archived data and making use of extra storage fields.

Table 3: SPRI RES Binary TRK file data record format (fields in red not used)

Record/field structure	**Data storage type**	**Field names**
struct TrackRecord	char	summary_of_N_waves; // indicates degree of waveform averaging against which picking performed
	double	Tx0_rawoffset; // point to which raw wave shifted back
	double	Tx0_offset; // point after zero at which first Tx rise starts
	struct TrackPoint	Track[4]; // Track surface, bed, alt sfc, alt bed
	struct MigPoint	true_horizon[2]; // Surface, Bed – not used
struct TrackPoint	double	Sample;
	bool	auto_tracked;

Record/field structure	Data storage type	Field names
struct MigPoint	double	max_hgt;
	double	min_hgt;
	double	hgt;

NB the information contained in the .TRK files is applicable to the NetCDF format radar data, as well as the original binary .DTA format data, albeit appropriate record offsets would need to be applied, depending on the Flightline part represented by NetCDF file.

NetCDF binary files

The SPRI Time-Tagged RES Profiles NetCDF data files contain fields as described in Table 4. Note, that pitch, roll and heading values were not recorded, and the fields are only present for compatibility with other radar data files (CReSIS / OIB / UTIG).

The digitizer DN values representing waveform amplitude are given in a field named amplitude_low_gain: this is in order to allow applications that read UTIG, etc. radar data to ingest the data without needing amendment for different field headings – the naming denotes no information regarding any actual gain setting. Since the data was only acquired in a single radar channel, there is no amplitude_high_gain field.

Table 4: NETCDF File Parameter Description

Parameter	Description	Units
time	Time of day, seconds since 1994-mm-dd 00:00:00, where mm and dd give date on which flight took place	UTC
fasttime	2-way travel time	Microseconds
lat	Latitude of sample	Decimal degrees North, WGS-84
lon	Longitude of sample	Decimal degrees East, WGS-84
altitude	Altitude of antenna above nominal sea level (WGS84)	Meters
pitch	Pitch of the platform. Positive is nose up. Zero is horizontal. NOT POPULATED	Degrees
roll	Roll of the platform. Positive is right wing up. Zero is horizontal. NOT POPULATED	Degrees
heading	Heading of the platform. Positive is clockwise from above. Zero is true north. NOT POPULATED	Degrees
amplitude_low_gain	Amplitude of radar reflection	Digitizer DN values
hae_gps	Height of antenna above WGS84 ellipsoid according to processed GPS record	Meters
hae_palt	Height of antenna above WGS84 ellipsoid according to processed pressure altitude record	Meters

Table 4: NETCDF File Parameter Description

Parameter	Description	Units
msl2hae	Height of geoid above ellipsoid (WGS84)	Metres

Sample Data Record

Below (Figure 3) are amplitude values from a sample of data file `SPRI1B2000095_CA_FLT01_SEG02_954877643_013.nc` as displayed in the HDFView tool.

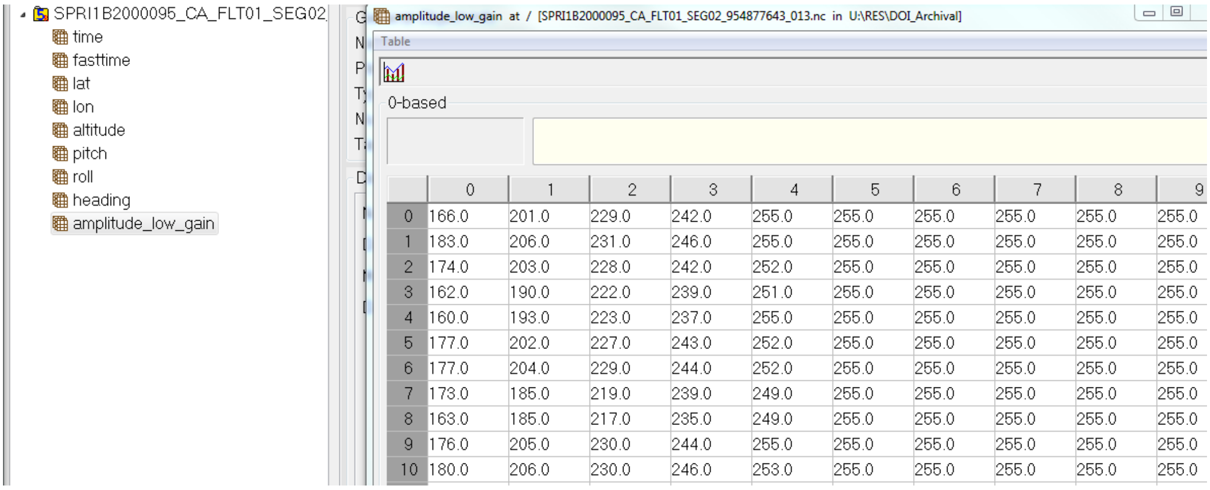

	0	1	2	3	4	5	6	7	8	9
0	166.0	201.0	229.0	242.0	255.0	255.0	255.0	255.0	255.0	255.0
1	183.0	206.0	231.0	246.0	255.0	255.0	255.0	255.0	255.0	255.0
2	174.0	203.0	228.0	242.0	252.0	255.0	255.0	255.0	255.0	255.0
3	162.0	190.0	222.0	239.0	251.0	255.0	255.0	255.0	255.0	255.0
4	160.0	193.0	223.0	237.0	255.0	255.0	255.0	255.0	255.0	255.0
5	177.0	202.0	227.0	243.0	252.0	255.0	255.0	255.0	255.0	255.0
6	177.0	204.0	229.0	244.0	252.0	255.0	255.0	255.0	255.0	255.0
7	173.0	185.0	219.0	239.0	249.0	255.0	255.0	255.0	255.0	255.0
8	163.0	185.0	217.0	235.0	249.0	255.0	255.0	255.0	255.0	255.0
9	176.0	205.0	230.0	244.0	255.0	255.0	255.0	255.0	255.0	255.0
10	180.0	206.0	230.0	246.0	253.0	255.0	255.0	255.0	255.0	255.0

Figure 3: Sample of low gain amplitude values.

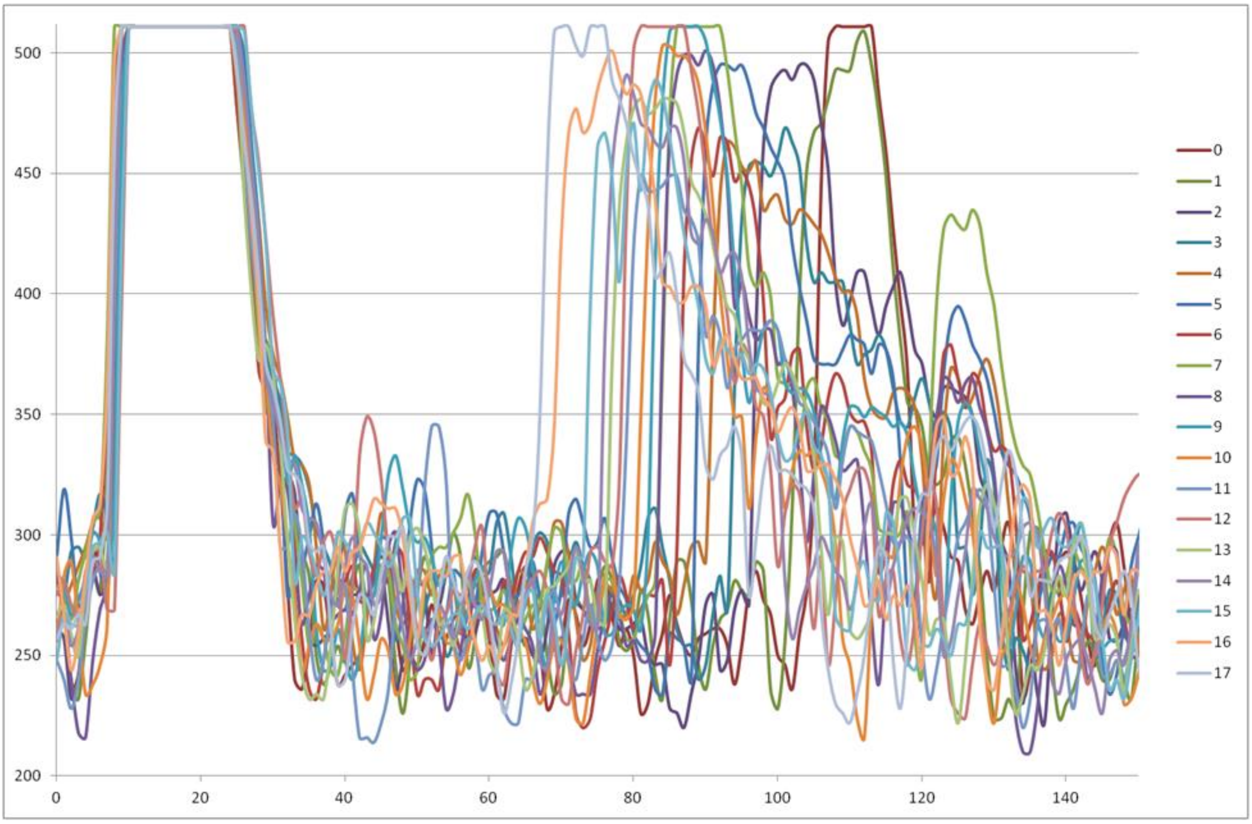

Figure 4: Plot of a number of waveforms. X-axis is 'fasttime' microseconds; Y-axis is digitizer DN number

Scott Polar Research Institute

File and Directory Structure

Data are located in the CA2000/RES/RAWDATA/ directory, within sub-folders applicable to the data format.

Folders contain NetCDF (.nc) files, and bespoke SPRI binary data (.DTA) and track (.TRK) files.

File Naming Convention

The data set NetCDF files are named according to the following convention and as described in Table 5:

SPRI1BYYYYDOY_CA_FLTnn_SEGss_ttttttttt_ppp.nc

Where:

Table 5: NetCDF File Naming Convention

Variable	Description
SPRI1B	Short name for SPRI L1B Time-Tagged Echo Strength Profiles
YYYY	Four-digit year of survey (1997)
DOY	Day of year of survey
CA	Geographic area
nn	Flight number within Project (01 – 11)
ss	Data Segment within flight.
ttttttttt	Original data file number, a 9-digit timestamp created from time of start of data acquisition, expressed as number of seconds since Reference date.
ppp	Part number (000 to # parts-1).
.nc	File type: NetCDF (.nc)

File name examples:

SPRI1B2000104_CA_FLT08_SEG01_955666991_012.nc

SPRI1B2000105_CA_FLT08_SEG04_955675582_000.nc

The corresponding SPRI Binary format files are named ttttttttt.DTA and ttttttttt.TRK, for RES data and interface tracking respectively (ttttttttt defined as in Table 1). E.g.:

955666991.DTA

955675582.TRK

File Size and Total data volume

Table 6: Data sizes

File Format	Extension	Size range	Total size[3]
NetCDF	.nc	approximately 1 to 20 MB	10.4 GB
SPRI Binary RES data	.DTA	~262 Kb to 138.4 MB	2.92 GB
SPRI binary track	.TRK	~45 Kb to 24.3 MB	519 MB
TOTAL main data			**13.63** GB
Other			
SPRI other binary	.GPS, .PAD, .PMN	~1KB to ~1MB	25MB
SPRI ancillary files	Various (.bmp, .zip, .dat, .dbf, .pdf, .txt, .tif, .bat)	~1KB to 13.3MB	860 MB
GPS raw files and processing	Various (.00n, .00o, .obj, .exe, .apr, .asc, .avl, .c, .zip, .cor, .dat, .dbf, .gif, .xls, .doc, .pdf, .pfb, .raw, .sbn, .sbx, .inf, .shp, .shx, .ssf, .txt, .y00, .Z)	~1KB to 12MB	192 MB
RES processing database files	.dbf, .krg, .mdx, .xls, .doc, .pos, .sql, .txt	~1KB to 43.2 MB	474 MB
RES processing ancillary images	.bmp, .png	7KB to 137 MB	626 MB
Derived Products (Shapefiles, etc.) and associated files	Various (.adf, .avl, .bmp, .zip, .cpg, .cpj, .dat, .dbf, .gif, .xls, .doc, .nit, .pdf, .prj, .rtf, .sbn, .sbx, .shp, .shx, .txt, .tif, .xml)	~1KB to 515 MB	1.70 GB
Archival software and general files	Various (.exe, .cbproj, .c, .h, .hpp, .cpp, .png, .xlsx, .pdf, .rtf, .bat	~2KB to 1.53 MB	5.63 MB
Acquisition and Processing software	Various (.exe, .bcb, .bgi, .bmp, .bpr, .h, .cpp, .dfm, .xls, .doc, .pdf, .res, .txt, .bat)	~1KB to ~2MB	259 MB
Total Other			**4.1GB**
TOTAL ALL			**18 GB**

Spatial Coverage

Canadian Arctic:

Northernmost Latitude: 81° 0' 32" N

Westernmost Longitude: 91° 12’ 46” W

Easternmost Longitude: 72° 8' 15" W

Southernmost Latitude: 74° 27' 57" N

[3] File sizes 1024-based

The target region for this glaciological data collection was the Canadian Arctic (CA), Queen Elizabeth Islands (QEI). Ice masses on Devon and Ellesmere islands were sounded. See Figure 5 for the overall flight track flown.

Acquisition of this dataset took place over the period 4th – 15th April 2000. In total, 11 survey flights took place, with a combined duration of ~45 hours, covering ~10,885 km. Figure 5 through Figure 9 illustrate specific locations for this dataset. Please see NC file attributes for details of geographical extent of each granule. Data-gathering legs (48) occupied ~29 hours of this flying time, over a flight track of ~7,150 km, with ice thickness measurements determined over ~3,600 km from the resultant data. Table 7 presents statistics regarding flight duration and data acquisition. Table 8 gives details of data-gathering flightlines within these, including specific glaciers or features covered and calibration legs.

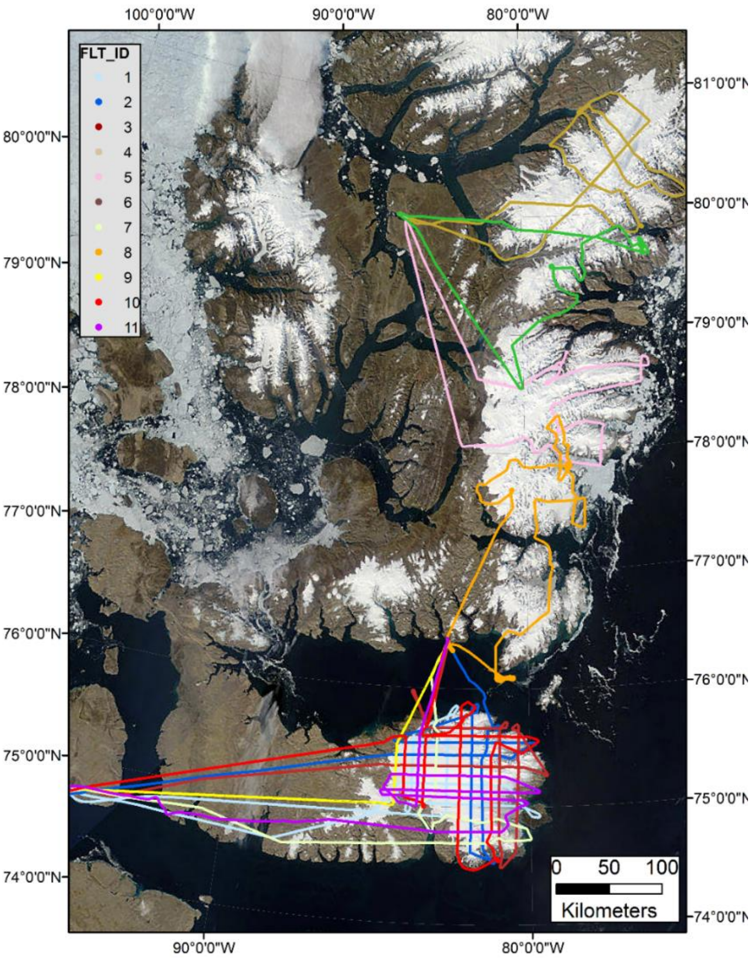

Figure 5: Flight tracks flown in the Canadian Arctic (CA) Queen Elizabeth Islands (QEI) archipelago 2000 airborne RES survey. The flight track is denoted in a different colour for each Flight. See following figures for further detail of data gathering sections.

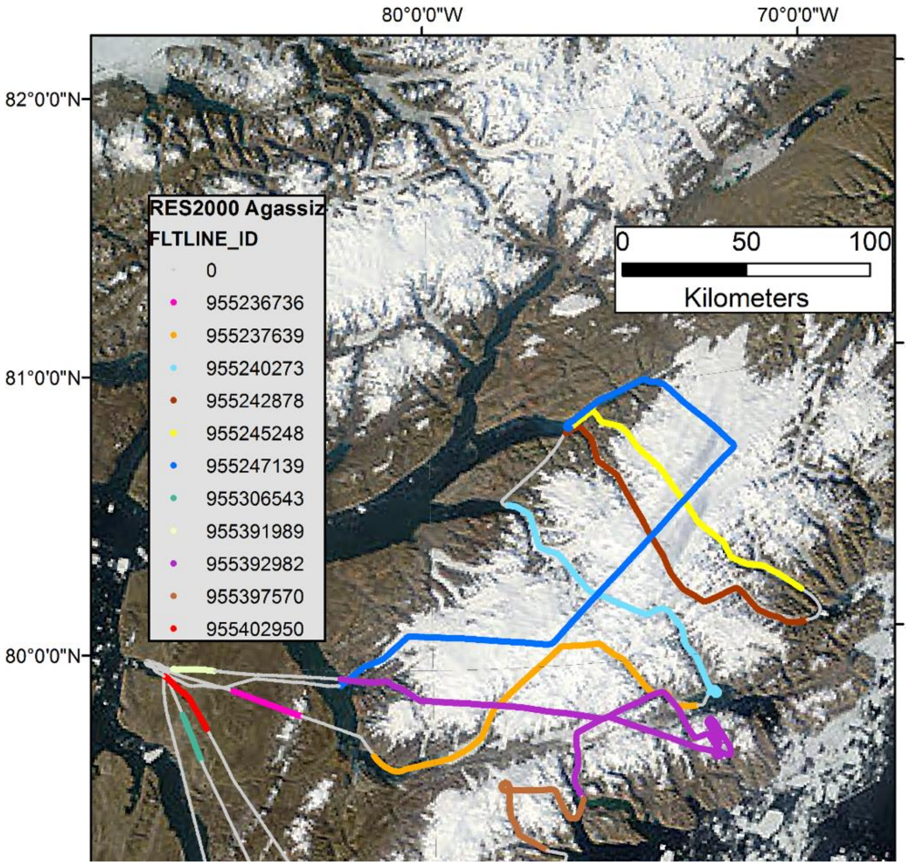

Figure 6: Data Legs (FLTLINE_ID) for Agassiz Ice Cap (Flown mainly out of Eureka)

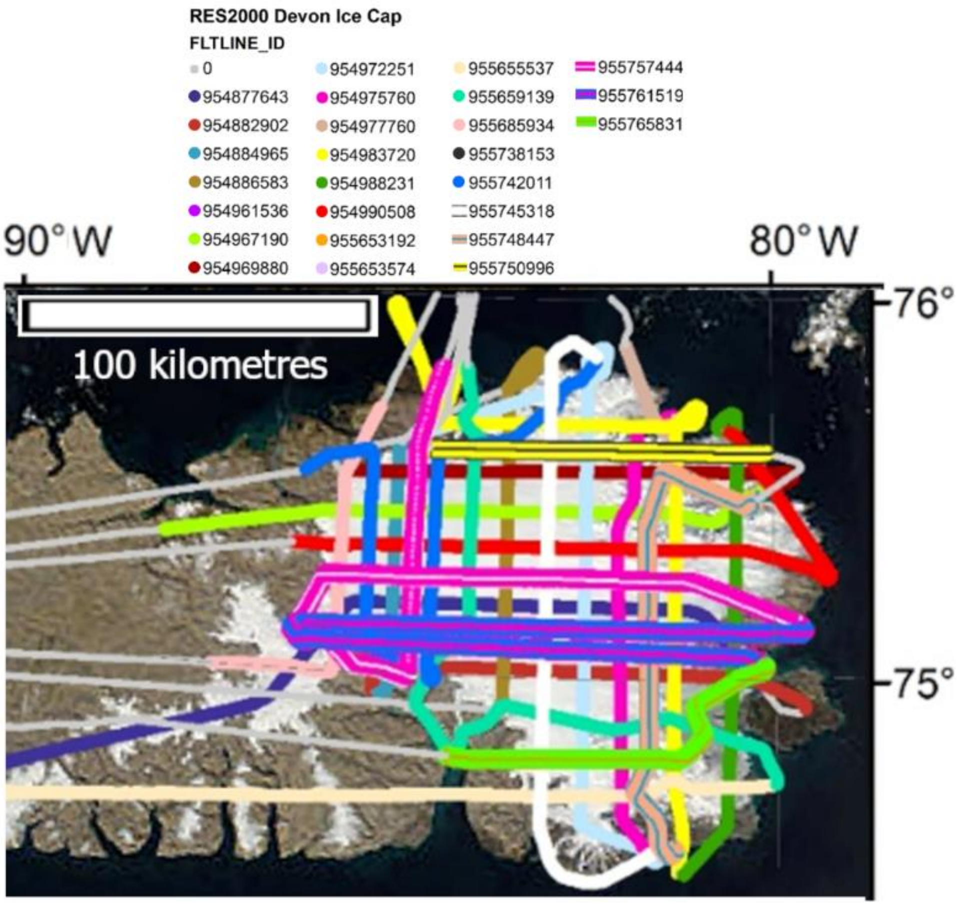

Figure 7:Data Legs (FLTLINE_ID) for Devon Ice Cap, flown mainly out of Resolute, with refueling stops at Grise Fiord

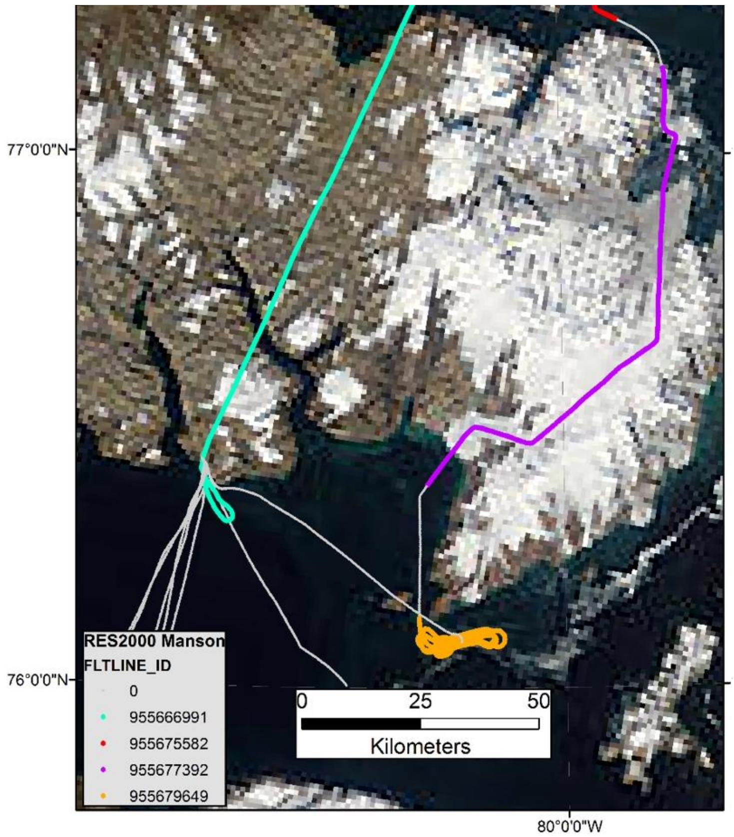

Figure 8: Data Legs (FLTLINE_ID) for Manson Ice Cap

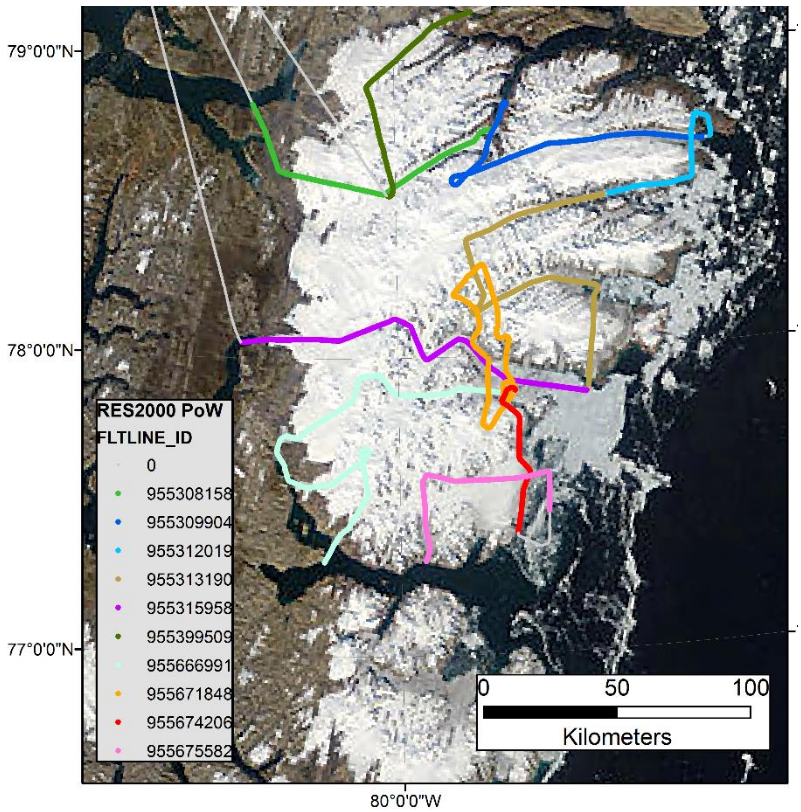

Figure 9: Data Legs (FLTLINE_ID) for Prince of Wales (PoW) Ice Field, flown mainly out of Eureka

Scott Polar Research Institute

Table 7: Statistics regarding Flight Duration and Data Acquisition

FLT	From	To	FLT km	Legs	Data Len km	Ithk Len km	Duration	Dta Duration
1	04/04/2000 19:13:12.750	05/04/2000 00:15:49.453	1223.03	4	690.2925	418.4756	5:02:37	2:45:51
2	05/04/2000 19:30:02.750	06/04/2000 00:04:43.781	1105.19	5	726.9355	422.8906	4:34:41	2:54:07
3	06/04/2000 00:53:23.906	06/04/2000 05:12:00.469	1043.29	3	666.129	308.6234	4:18:37	2:43:02
4	08/04/2000 23:22:20.375	09/04/2000 03:56:59.188	1105.37	6	879.9732	437.7703	4:34:39	3:36:09
5	09/04/2000 18:46:35.723	09/04/2000 23:08:30.992	1038.02	6	673.4233	323.7423	4:21:55	2:50:49
6	10/04/2000 18:33:31.547	10/04/2000 21:55:27.594	806.77	5	523.9722	175.259	3:21:56	2:11:37
7	13/04/2000 19:05:40.156	13/04/2000 22:15:46.750	767.07	4	532.4475	239.4925	3:10:07	2:08:22
8	13/04/2000 22:59:49.469	14/04/2000 03:28:55.375	1080.35	6	934.9951	300.751	4:29:06	3:45:41
9	14/04/2000 03:53:19.656	14/04/2000 05:55:08.188	479.90	1	115.67	68.29462	2:01:49	0:27:51
10	14/04/2000 18:40:19.719	14/04/2000 23:12:59.344	1115.78	5	718.4465	421.5321	4:32:40	2:54:52
11	14/04/2000 23:49:12.344	15/04/2000 04:24:38.938	1120.51	3	689.627	486.7532	4:35:27	2:46:48
TOT			10885	48	7152	3603	45:03:34	29:05:09

Table 8: Data Gathering Flightlines for survey flights

FLT	FLID	Description / Area Covered	Sections of specific interest (records from-to)
-	954870658	Calibration of digitizer DN vs input radar Short Pulse (SP) signal dB attenuation	SP000 (10-800) SP010 (1025-1725) SP020 (1925-2650) SP030 (2900-3600) SP040 (3825-4550) SP050 (4800-5475) SP060 (5700-6375) SP070 (6600-7275) SP080 (7650-8200) SP090 (8525-9200) 'nnn' = added attenuation in dB
-	954870898	Calibration of digitizer DN vs input radar Long Pulse (LP) signal dB attenuation	LP000 (10-775) LP010 (1050-1750) LP020 (1975-2675) LP030 (2900-3675) LP040 (3900-4675) LP050 (4775-5600) LP060 (5750-6550) LP070 (6725-7475) LP080 (7650-8425) LP090 (8625-9425) LP100 (9725-10225) LP110 (11075-11575) 'nnn' = added attenuation in dB
1	954877643	Devon Ice Cap	Sea Level info (157297-169437) Hyde Inlet N (227090-245450) Sea Level - End FL954877643 (250734-251976)
1	954882902	Devon Ice Cap	Sea Level - Start FL954882902 (13459-14338) Hyde N(3) (16180-33182)
1	954884965	Devon Ice Cap	Northern glacier 3 (34190-54560)

FLT	FLID	Description / Area Covered	Sections of specific interest (records from-to)
1	954886583	Devon Ice Cap	Sea Level - Start FL954886583 (14520-16805) onto N of icecap (20300-26375) Northern glacier 7 (22490-56980)
2	954961536	Devon Ice Cap	
2	954967190	Devon Ice Cap	Sea Level info (26897-48817) NW (34180-84090) NE (84090-123320) Outlet bet FitzRoy/Raper(S) (107860-123175) Sea Level - End FL954967190 (131046-133086)
2	954969880	Devon Ice Cap	Sea Level - Start FL954969880 (120-2240) NE (9720-57140) NW (57140-95310) Sea Level (87850-96108)
2	954972251	Devon Ice Cap	Crossing Point (CP) at N vs 954886583 (18191-25151) cross glacier in NE (30385-40044) Sea Level - First part FL954972251 (42843-52418) W of Cunningham W (149613-165593) Sea Level - End FL954972251 (165422-175177)
2	954975760	Devon Ice Cap	Sea Level - Start FL954975760 (10-450) GH_crossing (280-93870) Cunningham West Glacier (510-16515) above Cunningham W (24060-30780) CP187 (25907-30757) bed gap S of ridge (54876-59714) Belcher Glacier (69170-93175) Sea Level - End FL954975760 (93821-98854)
2	954977760	Devon Ice Cap	Sea Level - Start FL954977760 (70-7354)
3	954983720	Devon Ice Cap	Sea Level - Start FL954983720 (100-4534) NE outlet (100350-105925) NE topo (129582-159913) Sea Level - End FL954983720 (221597-224726)
3	954988231	Devon Ice Cap	Sea Level - Start FL954988231 (75-9125) Sea Level - End FL954988231 (101308-112266)
3	954990508	Devon Ice Cap	Sea Level - Start FL954990508 (55-2030) Bowles Bay (45145-77950) NE_3 (45530-104820) across EW (45660-149040) up glacier E side (45790-63963) centre icecap (92657-105132) NW_3 (104820-149120) Sea Level (137056-152175)
4	955236736	Agassiz Ice Cap	
4	955237639	Agassiz Ice Cap	Sea Level - Start FL955237639 (9290-21090) Cañon outlet (22460-64849) Eugenie N (90660-124790) Eugenie N common W (110519-125704)
4	955240273	Agassiz Ice Cap	Sea Level - Start FL955240273 (35-10645) Dobbin Bay Glacier (10870-53336) D'Iberville Glacier (61853-96410) Sea Level - End FL955240273 (96565-100431)
4	955242878	Agassiz Ice Cap	Up Glacier (1685-38304) Sea Level - Start FL955242878 (2190-2540) Antoinette Glacier (5000-41807) John Richardson Bay S Glacier (61962-102040) Sea Level - End FL955242878 (103923-104143)
4	955245248	Agassiz Ice Cap	Sea Level - Start FL955245248 (1650-1815) up outlet glacier from John Richardson B (4250-36838) SW end Lake Tuborg (66954-89950)
4	955247139	Agassiz Ice Cap	Sea Level - Start FL955247139 (2675-6150) Tuborg Floating Tongue (6445-14250) mirror (24351-24436) mirror2 (26776-27181) outlet North end of Lake Tuborg (32410-50920) outlet Agassiz SW #2 (N) (171904-198440) Sea Level - End FL955247139 (202656-203181)
5	955306543	Agassiz Ice Cap	
5	955308158	Prince of Wales Ice Field	WNW PoW to Top of Stygge (22430-46200) Cross divide 1 (33717-55202) Stygge glacier (46310-83240) sea level end FL (84015-85880)
5	955309904	Prince of Wales Ice Field	sea level start FL (8479-9784) Stygge S (9730-27730)

FLT	FLID	Description / Area Covered	Sections of specific interest (records from-to)
			L0 (24505-61220) Stygge SE top (46310-52585) Leffert glacier (60804-102450) Sea Level - End FL955309904 (103786-104146)
5	955312019	Prince of Wales Ice Field	Sea Level - Start FL955312019 (15-1345) across Leffert snout (16430-30361) Leffert Glacier across snout (16530-19550) Jewel Glacier across (19550-25700) Alfred Newton Glacier across (27410-30290) MacMillan glacier (37080-51092)
5	955313190	Prince of Wales Ice Field	Over sea - start FL 955313190 (65-645) Ekblaw Glacier (1700-44772) crossing (60000-67425) Cadogan Glacier (67306-104170) Sparks Glacier (109112-135976) Sparks North (109770-123731) Sparks South (123730-135000) Over sea end FL 955313190 (136738-136983)
5	955315958	Prince of Wales Ice Field	Sea Level - Start FL955315958 (6150-27345) Trinity Glacier (27480-76967) Outlet to Vendom Fiord (88611-107840)
6	955391989	Agassiz Ice Cap	
6	955392982	Agassiz Ice Cap	Sea Level - Start FL 955392982 (1230-1605) Agassiz SW Outlet #1 (S) (16680-35126) Parrish glacier (mid) (82060-89985) Eugenie Glacier W (82063-113610) Eugenie W common N (101102-113631) John Evans (122430-173998) CPs B (131055-140509) CPs A (164674-167133) Parrish Glacier (lower) (196142-225480) test section (221736-224136) Sea Level - End FL955392982 (227239-227654)
6	955397570	Agassiz Ice Cap	Sea Level - Start FL955397570 (140-1215) Sven Hedin Glacier (9230-27421) Benedict Glacier (42620-63530) Sea Level - End FL955397570 (63769-66505)
6	955399509	Prince of Wales Ice Field	NW PoW (11340-44250) Cross divide 2 (46346-69267)
6	955402950	Agassiz Ice Cap	2000' P-alt 29.92 over fiord FL 95540295 (15010-15845)
7	955653192	Devon Ice Cap	
7	955653574	Devon Ice Cap	
7	955655537	Devon Ice Cap	Sea Level - End FL955655537 (177845-179592)
7	955659139	Devon Ice Cap	Sea Level - Start FL955669139 (320-9215) Floating Tongue Query (7769-12034) Devon SE Interior (26840-59625) CP187 (42274-47114) CP69 (64122-69032) E Glacier into Croker Bay (72688-88725) Sea Level - Mid FL955669139 (89706-104431) outlet glacier S of icesheet (105753-126226) W Glacier into Croker Bay (105955-126310) North 6 (149690-183940) Sverdrup Glacier (164624-183810) Outlet at north (164874-184084) Sea Level - End FL955669139 (187026-189072)
8	955666991	Prince of Wales Ice Field; Manson Ice Cap	Palisade Glacier (100670-124552) Hook Glacier (133115-155250) Split Lake Glacier (169050-194984) Wykeham Glacier (198807-240810) Sea Level - End FL955666991 (240935-242950)
8	955671848	Prince of Wales Ice Field	Sea Level - Start FL955671848 (50-2590) FL 955671848 - Iceberg Sounding (11035-13455) Talbot Glacier (19747-47292) Trinity Glacier North (47250-94500) Trinity (N) Glacier +Wykeham+ (47645-103895) Small glacier S of Trinity (94500-104720) NE Inglefield outlet (104990-115460) Sea Level - End FL955671848 (116815-117165)
8	955674206	Prince of Wales Ice Field	Sea Level - Start FL955674206 (4040-4505) Across SE PoW Shelf (4720-46339) Sea Level - End FL955674206 (46205-46675)

FLT	FLID	Description / Area Covered	Sections of specific interest (records from-to)
8	955675582	Prince of Wales Ice Field; Manson Ice Cap	Sea Level - Start FL955675582 (1405-1770) Shelf Outlet to Cape Mouat (11450-47002) Outlet to Makinson Inlet (49446-72470) Sea Level - End FL955675582 (78342-78662)
8	955677392	Manson Ice Cap	Cape Stokes across 2 outlets (20-7550) Sea Level - Start FL955677392 (12915-13105) Smith Bay Outlet Glacier (19850-50044) Jakeman Glacier (50884-85830) Sea Level - End FL955677392 (91502-91622)
8	955679649	Manson Ice Cap; Radar system calibration looping over polynya at various 1000 ft separations; attenuations; bank angles.	Double bounce cal (21-412) 2000ft (7495-10555) 2000ft 10dB attenuation (17799-24518) 2000 sea level (22959-23409) 3000ft 10dB atten (34124-37104) 3000 sea level (35624-36059) 4000 sealevel (45214-45779) 4000ft 10dB atten (45669-50239) 5000ft 10dB atten (57084-62449) 5000 sea level (60934-61329) 6000ft 10dB atten (75159-82124) 6000 oversea (75801-76376) 6000ft 10dB atten bank angle 20 degrees (82954-88454) 6000ft 10dB atten bank angle 30 degrees (89424-93429) 6000ft 10dB atten bank angle 45 degrees (94369-96179)
9	955685934	Devon Ice Cap	Sea Level (8113-45297) North 1 (16810-31840) Crossing (59230-72950)
10	955738153	Devon Ice Cap	
10	955742011	Devon Ice Cap	Sea Level (865-51359) North 2 (16660-37400) S of icesheet outlet glacier crosspt (64374-85423) North 5 (105300-128030) Sverdrup Glacier (W-E S end) (121321-138311) Outlet glacier at end of FL (139602-163638) Eastern Glacier, N Devon (139888-163105) Sea Level - End FL955742011 (163243-165398)
10	955745318	Devon Ice Cap	Sea Level - Start FL955745318 (10630-14000) North 8 (16140-56840) CP69 (89021-92991) Sea Level - End FL955745318 (150177-150397)
10	955748447	Devon Ice Cap	Sea Level - Start FL 955748447 (4450-4780) Phoenix Head Glacier (6741-21776) Above Phoenix Head (22035-35990) Sea Level - End FL955748447 (105769-107159)
10	955750996	Devon Ice Cap	Sea Level - Start FL955750996 (15-770)
11	955757444	Devon Ice Cap	Sea Level - Start FL955757444 (20-1300) North 4 (19600-41520) CP121 and CP122 (57074-63059) Sea Level (98893-120307) On to W Devon ice (0-105740) across ice cap (107260-200190) Hyde North(2) (180785-200095) Sea Level - End FL955757444 (201026-201336)
11	955761519	Devon Ice Cap	First leg across DIC (490-112174) Sea Level - Start FL955761519 (3961-4356) CP141 and CP122 (82887-89232) Second leg across DIC (111869-214756) CP121 (137534-144284) Sea Level - End FL955761519 (214751-214881)
11	955765831	Devon Ice Cap	Sea Level - Start FL955765831 (3491-3816) Hyde North(4) (5233-23233) SE interior S of nunatak (23338-59768) Sea Level - End FL955765831 (81974-82204)

Spatial Resolution

The flights were at a nominal air speed of ~230 km hr^{-1} and were flown at a constant pressure altitude, which ranged from 700 to 1100 m, depending on weather conditions. Processed radar soundings are given at ~50 Hz (20 milliseconds) which is roughly 1.3 m apart depending on platform velocity. Vertical samples (fast time) are given at 20 MHz (50 ns fast time). This is approximately 7.5 meters in air (using a standard velocity value of 300 m μs^{-1}) and 4.2 meters (168 m μs^{-1}) in ice (two-way travel time).

Projection and Grid Description

Latitude, longitude, and altitude above sea level are provided with respect to the WGS84 reference. Flight tracks are as shown in Figure 5.

Temporal Coverage and Resolution

The data were all acquired in a single April 2000 field campaign, funded by NERC grant GR3/12469, and by the EU SPICE Project to Julian Dowdeswell, as well as by grants from the Meteorological Service of Canada (CRYSYS program) to Martin Sharp.

Parameter or Variable

Parameter Description

Ice thickness data products

Ice thickness point measurements (All)

Surface elevation, ice thickness, and bed elevation values were extracted for the entire dataset at a nominal spacing of 20 metres, with average values summarized at extraction points within a radius of 10 metres. These are given in tab-delimited ASCII text files, and as an ESRI Shapefile.

Gridded ice thickness and elevation products (Devon Ice Cap)

Grids of surface elevation, ice thickness, and bed elevation were generated at a 1 km posting size, in UTM Zone 17N, WGS84 projection. These were collected – together with input and ancillary files – on a CD, copies of which were shared with a number of collaborating researchers. The production process and data files are described in a separate document included with the data in a sub-folder ‘CD’.

Ancillary data

See under Gridded data description

Software and Tools

Data Acquisition, Processing and Viewing software

Code was produced in C/C++, within a Borland C++ Builder 4 IDE[4], for data acquisition software (and associated utilities) and for working-up, viewing and analysis of RES and associated data acquired. ***The source code for this software is provided within this archive as an ancillary record to the main RES dataset, with no warranty, instruction or further documentation provided.*** Any use of this code by others is at their own risk, and their own responsibility.

The data acquisition software makes use of freeware code from Chi-Hao Tsai available from the Internet at technology.chtsai.org/pctimer/ (as at 13 Dec 2017) in the implementation of a millisecond resolution timer.

Figure 10 illustrates the applications for which code is provided. The main application used in data acquisition is **acquire.exe**. This provides a simple keystroke user interface for the control of data acquisition - including the starting and ending of data legs – which provides a playback of acquired data in Z- or A-scope mode. It stores copies of data on three devices: two independent hard disks, and one RAM store (as backup in case of HD failure / temporary outage). Data files are kept to a maximum size of ~10MB, to facilitate transfer of data from the aircraft. Application **zippy.exe** is used to copy files from acquisition PC disks to ZIP disk, maintaining a list of files and of their transfer status.

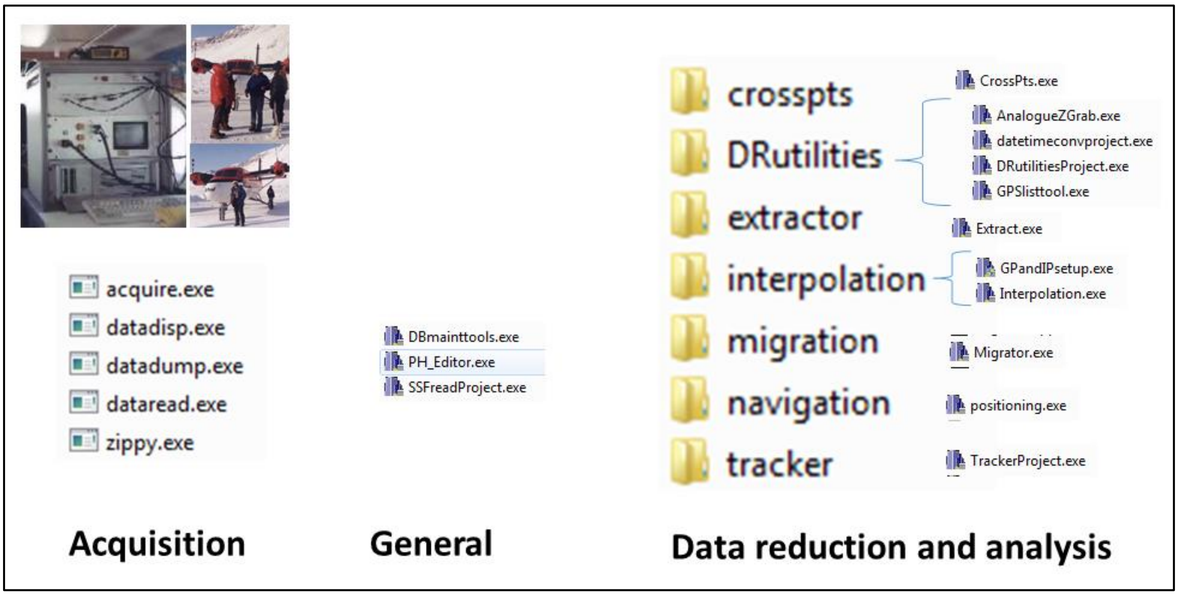

Figure 10: Applications related to the RES data acquisition and processing for which source code is available

The main RES data viewing and interface tracking analysis activities were supported by the **TrackerProject.exe** application. This software allows the display of RES profiles in Z-scope (raw, differentiated or start-of-rise points) and A-scope (single waveform) views, as well as showing corresponding flight track over plan-view satellite imagery. See Figure 11.

[4] Now Embarcadero C++ Builder

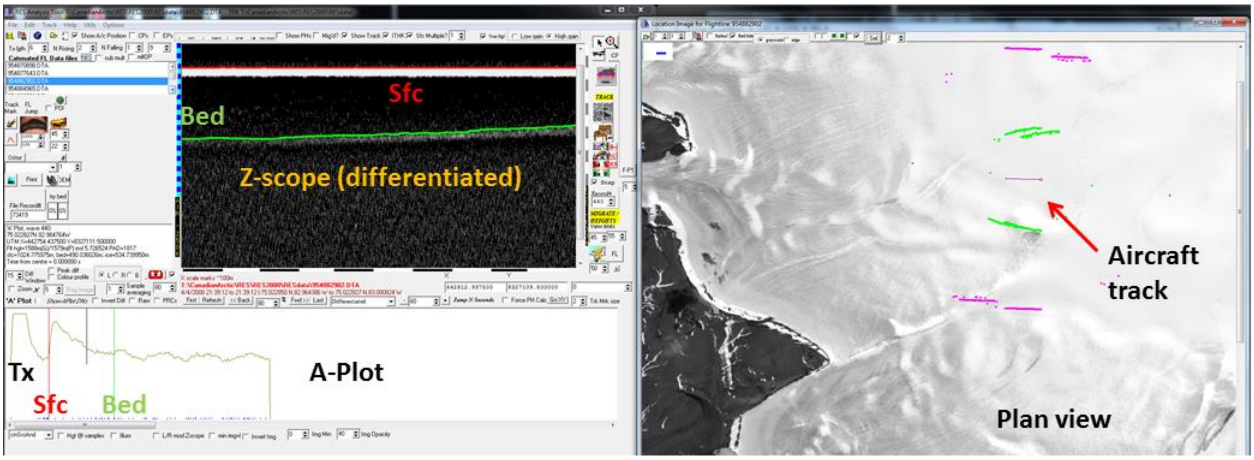

Figure 11: Example TrackerProject display

Note that, the TrackerProject application underwent revision during (and beyond) the original project duration, with experimental features tried out along the way – other than core display, tracking and extraction capabilities, all should be treated as 'unfinished'/'experimental'. The code archived here represents a stage of development encompassing the original data working (the application has since undergone update, to ingest other format data, and its functionality extended).

Other utility applications include CrossPts.exe, for analysis of differences in surface / bed elevation and ice thicknesses at flightline crossover points, and **Interpolation.exe**, used for Devon Ice Cap thickness grid interpolation (along with **GPand IPsetup.exe**, for setting up of Input Point, and output Grid Point data required by interpolations).

NetCDF file access and viewing

The following links provide access to software for reading and viewing NetCDF data files. Please be sure to review instructions on installing and running the programs.

- See the NetCDF Resources at NSIDC page (nsidc.org/data/netcdf/tools.html, as at 6 Dec 2017) for tools to work with NetCDF files.
- HDFView: Visual tool for browsing and editing HDF4, HDF5, and NetCDF files, available from The HDF Group (www.hdfgroup.org, as at 6th Dec 2017).
- ncBrowse (www.pmel.noaa.gov/epic/java/ncBrowse/, as at 6th Dec 2017)

NetCDF files were generated from CDL text files, using utility program **ncgen**. In order to generate the CDL files, the relevant header fields and waveform data were first extracted to ASCII text from the SPRI raw waveform data files. This information was then reformatted and combined with metadata to produce the CDL files. Software code and batch command files are given in the general section of this archive, along with an associated README file explaining the process in greater detail.

Data Acquisition and Processing

Theory of Measurements[5]

Ice is nearly transparent at Very High Frequency (VHF) radio frequencies (Dowdeswell and Evans, 2004). The radar operates by transmitting a radio frequency signal and receiving the time delay and power of the returning echo. For airborne sounding of ice, antennas direct energy to nadir. Through repeated pulses and motion of the aircraft, a radargram, a profile of power in time delay versus transmit time coordinates, can be mapped out. From the time delay between transmission and reception, and knowledge of the refractive index of ice (1.78), range to the bed can be estimated. The power of reflection relates to the dielectric contrasts between media and the roughness of the interface.

Data Acquisition Methods

Acquisition equipment setup and operation

Data were acquired from Radar, GPS and Pressure Transducer instruments via the program **acquire.exe** (see software section), running on an Arcom industrial rackmount Pentium PC, with DOS operating system. The acquisition PC was equipped with a GaGe / Compuscope CS220 digitizer card, used to perform analogue-to-digital sampling of radar waveforms, and an Arcom PCAD12/16H card for pressure sensor readings. An RS232 serial link was used to receive ASCII position report messages from the Trimble single-channel GPS receiver at start and end of each Flightline (for time synchronization); GPS positions were recorded by the GPS receiver itself every ~6 seconds. See Figure 12 for an illustration of the acquisition equipment mounted within the Twin Otter cabin, and of an under-wing half-wave (i.e ~1.5 m) dipole antenna. Two antennae were mounted – one under each wing at a quarter-wave distance, i.e. 0.75 m – for Transmit (Tx) and Receive (Rx) of radar energy.

[5] Text in this section from nsidc.org/data/IR2HI1B

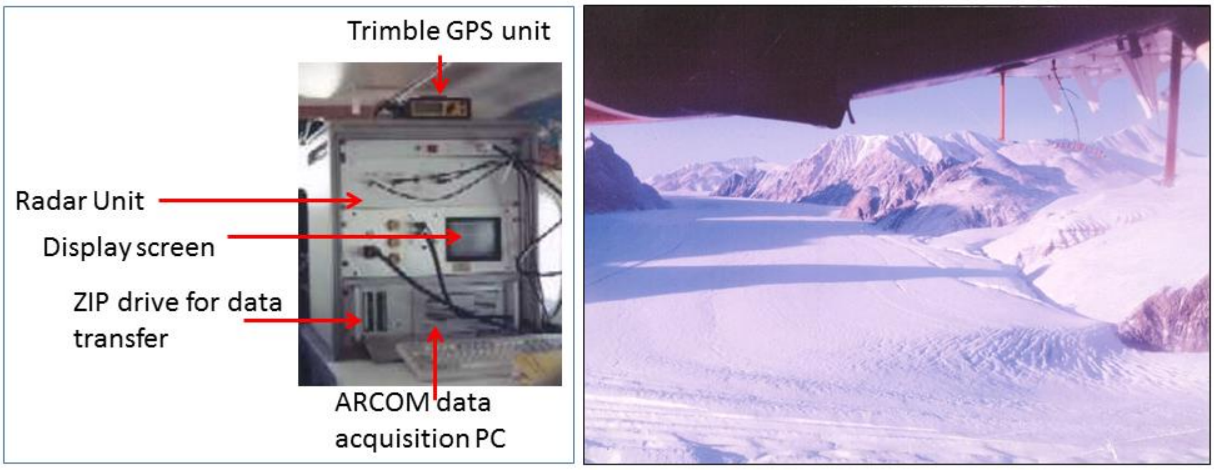

Figure 12: Radar, GPS and Data Acquisition equipment mounted (left) within Twin-Otter aircraft, and (right) under-wing half-wave dipole antenna.

Radar and waveform digitization parameters are as given below in Table 9.

Table 9: Radar and Waveform Digitization parameters

Parameter	**Value**
RADAR parameters	
Radar	SPRI radar, designed by Michael Gorman
Frequency	100 MHz
Center Wavelength in Air	2.99792458 m
Pulse Power	1 kW (long pulse) / 0.25 kW (short pulse)
Pulse Length	0.3 microseconds Short / 1.1 microseconds Long
Receiver Sensitivity	-125 dB
Receiver Noise	6 dB
Performance	150 dB Short pulse, 160 dB Long pulse (excluding antenna gain)
Receiver path	Successive detection log amplifier
Digitization parameters	
Digitizer	CompuScope 220 Ultra-Fast ISA Analog Data Acquisition Board
Digitizer manufacturer	DynamicSignals / GaGe
Digitizer platform	ARCOM Industrial Rackmount Pentium PC running MS DOS.
Sample rate	20 MHz (50 ns intervals)
Record duration	25.6 microseconds (512 samples)
Record rate	~50 Hz
Channels	2
Digitization	8 bit. No stacking.
Data rate	25.6 Kb/sec
DN to dB (SP)	Short pulse dB loss: $dB = 0.0044DN^2 - 2.6016DN + 457.13$ (R^2 0.9946)
DN to dB (LP)	Long pulse dB loss: $dB = 0.0068DN^2 - 3.6512DN + 598.94$ (R^2 0.997)

Table 9: Radar and Waveform Digitization parameters

Derivation Techniques and Algorithms

Processing Steps

Radar data

Data file segments (limited to ~10Mb size, to allow for transfer from aircraft) were concatenated, with waveforms shifted back to align at the start of Tx power rise). Data were not stacked, other than dynamically during data display and interface tracking.

Positioning Data

Trimble Pathfinder Office Version 2.51 software was used for Differential Post-Processing Correction of our GPS Rover Raw SSF data files. Since we were using older model GPS receivers with single carrier frequency, and due to data format limitations, we were unable to make use of other facilities to try to improve the accuracy of differential correction (e.g. application of ionospheric / tropospheric corrections or use of precise epheremides). Unfortunately, the timing of our survey meant that GPS data were still subject to the Selective Availability random error introduced into GPS signals (this random error feature was turned off in May 2000).

Lack of differential processing Base station data coverage for our uncorrected GPS Rover data meant that we had to produce a ‘master’ set of position data by reconciling three sets of point data. These points were differentially-corrected using: a) our own (Resolute / Eureka) Base receiver data; b) Thule Base receiver data; and c) (limited) Base receiver data from Liz Morris’ Devon Ice Cap base location (Differential correction results indicated comparable accuracies). For each raw GPS position, the differentially-corrected point sources were considered in preferred order: Thule; Devon, Resolute/Eureka.

Table 10 Summary of GPS Differential Correction Point Confidence Values

		XY				Z			
	confidence	average	max	min	stddev	average	max	min	stddev
Resolute/ Eureka	68%	2.513497	5.271	1.917	0.501348	5.466286	11.347	0.18	2.270111
Cover 57.51%	95%	5.026985	10.543	3.834	1.002701	10.93258	22.694	0.36	4.540208
10407 points	99%	7.540464	15.814	5.752	1.504046	16.39885	34.041	0.539	6.810323
Devon	68%	2.321925	3.702	1.83	0.385	4.179939	10.892	0.138	2.24066
Cover 6.79%	95%	4.643832	7.404	3.66	0.769996	8.359873	21.784	0.275	4.481347
1228 points	99%	6.965722	11.106	5.49	1.155006	12.53979	32.676	0.413	6.722
Thule	68%	2.556	5.530	1.924	0.467	5.506	11.380	0.403	2.035
Cover 92.93%	95%	5.111674	11.06	3.847	0.933392	11.01225	22.76	0.807	4.069
16816 points	99%	7.667507	16.59	5.771	1.400093	16.518	34.14	1.21	6.103881

Table 10 Summary of GPS Differential Correction Point Confidence Values

The GPS Z value record of height was more variable in quality than the XY values. We thus employed a 'voting' algorithm to select the most credible Z value from the available GPS sources. Where more than one sources’ Z values agreed within 5 metres, the average of these values was taken; if all sources’ Z values were more than 5 metres apart, then the sources were considered in preferential order (best first): Devon, Thule, Resolute/Eureka, Raw. The number of 'votes' obtained by the Z value derived for each position was recorded as a quality indicator.

A rolling average (of five) GPS Z values was calculated along each FL (avoiding time gaps) to smooth out periodic sinusoidal fluctuations (assumed to lie around a mean) observed in individual point source data, and to even out any potential artefacts of the voting process. This was the value used in subsequent RES position tagging and other processes.

Time offsets were calculated between acquisition PC timestamps and GPS time/position details obtained via serial link at start and end of each Flightline. These time offsets were employed in the tagging of RES data with GPS positional information. There were difficulties with offset determination due to the whole-second precision of the GPS time messages and some serial link interface problems.

An inaccuracy of one second would contribute around sixty to seventy metres to XY positional error budget, although visual inspection of RES record versus location on (ortho-rectified) ETM+ imagery in several locations indicated good agreement. Similarly, comparison of sloping GPS and pressure records indicated good agreement, as did Cross Point analysis (see **Table 11**). We therefore assumed a half-second worst-case error.

Due to problems in the GPS Z record (including some drop-out or nonsensical values), the aircraft elevation adopted for subsequent processing (including surface elevation calculation) was set according to a pressure transducer data number value obtained and stored concurrent with each RES waveform acquisition. To avoid any 'spikes' in the pressure DN record, a rolling average DN value was calculated for each waveform.
DN-to-Height relationships (slope and offset) were determined at a number of 'pinning points', including over-sea calibration legs and areas of credible GPS Z record. The use of GPS-derived pinning points was necessitated by the observation that sea-level calibration intercepts are non-constant spatially and temporally and that the accuracy of the Pressure DN-to-height relationship may be compromised (e.g. by phenomena such as katabatic winds streaming down outlet glaciers) in over-ice areas between sea-level calibrations. There was often a large spatial separation between sea-level calibration sections, and furthermore these calibrations provide no information about pressure behaviour over the ice itself (which was observed to differ greatly from GPS Z value).

Without independent means of comparing our GPS and Pressure-derived height values, it was necessary to compare the data from the different sources with a view to establishing the most credible and consistent values. This process was guided by intermediate results of cross-point analysis used to check that addition or removal of pressure pinning-points did not degrade surface cross-point agreement. Pinning-points were not added directly at crossing points, and we sought to ensure that pinning-points had a rationale with respect to other supporting data (i.e. GPS) and were not added simply to better cross point agreements. GPS data were inspected and flagged as necessary to avoid 'bad data' sections where the GPS Z value was repeated consecutively (indicating a drop-out from 3D mode). Comparison with a handful of GPS points obtained very accurately on the surface of the Devon Ice Cap (Douglas Mair) and lying very close to our sub-aircraft track also aided in assuring accuracy of pressure-derived heights.

By using the pressure-height offset values closest in time to RES waveform acquisition, a pressure-derived height was calculated for (and stored in the header of) each waveform record. The nearest (in time) pinning values were found before and after each waveform and pressure-height relationship parameters interpolated according to linear time distance.

Positional and Interface Tracking Accuracies

In order to check the quality of navigation and horizon tracking, we assessed the level of agreement at flight line crossover points (CPs). These were generated by locating the RES waveform records from pairs of FLs nearest to the point at which the lines cross. The tracked surface and bed horizons and ice thickness (surface elevation minus bed elevation) were summarized for each FL within a 20 m radius of these CPs and values compared. Individual crossing point mean value difference statistics were further collated to produce the overall difference statistics quoted in **Table 11**. 'N' is the number of CPs for which data could be summarized from both crossing FLs. Statistics were generated firstly over all defined CPs and then excluding those outlier CPs exhibiting an error beyond the overall mean error by more than two standard deviations. Figure 13, Figure 14 and Figure 15 show the distribution of CP differences, binned at 5m intervals.

Table 11 Crossing Point Analysis Summary Statistics

Surface Differences Statistics

		N	Mean	Median	Max.	Min.	StdDev	Commentary
Surface:	Overall	165	7.69	6.17	32.48	0.01	6.35	Reasonable accuracy, with all bar 10 within 20m
	Main	114	8.00	6.42	31.35	0.01	6.41	
	Outlets	24	7.74	7.09	20.61	0.09	5.59	
	Land	10	9.87	5.94	32.48	2.46	9.35	Land further from sea calibration and rougher non-ice topography?
	Sea	17	4.26	3.39	13.74	0.18	3.68	Best accuracy over sea, as expected due to proximity to pressure calibration. Errors from icebergs, etc?
Surface without Outliers:	Overall	155	6.61	5.69	18.62	0.01	4.73	
	Main	108	7.06	6.17	18.62	0.01	4.70	
	Outlets	23	7.18	6.81	17.86	0.09	4.98	
	Land	9	7.36	5.61	17.45	2.46	5.24	
	Sea	16	3.67	2.97	9.33	0.18	2.84	

Bed Differences Statistics

		N	Mean	Median	Max.	Min.	StdDev	Commentary
Bed:	Overall	116	11.01	8.32	131.76	0.10	14.17	Error dominated by single outlet CP. Combination of surface + thickness errors.
	Main	100	10.12	8.21	44.45	0.10	8.79	
	Outlets	16	16.56	9.74	131.76	0.72	31.49	
Bed without Outliers:	Overall	114	9.65	8.03	31.30	0.10	7.97	
	Main	92	8.27	7.15	24.02	0.10	6.21	
	Outlets	15	8.88	8.81	30.91	0.72	7.18	

Ice Thickness Differences Statistics

		N	Mean	Median	Max.	Min.	StdDev	Commentary
Ice thickness:	Overall	116	7.52	4.84	131.39	0.01	13.09	Error dominated by single outlet CP.
	Main	100	6.25	4.78	31.85	0.01	6.11	
	Outlets	16	15.47	8.62	131.39	0.48	31.47	
Ice thickness without Outliers:	Overall	115	6.45	4.78	31.85	0.01	6.10	Other than four points, within 20 m.
	Main	96	5.47	4.53	17.39	0.01	4.52	
	Outlets	15	7.74	6.13	19.33	0.48	6.12	Slightly higher outlet values due to more complex topography?

Table 11 Crossing Point Analysis Summary Statistics

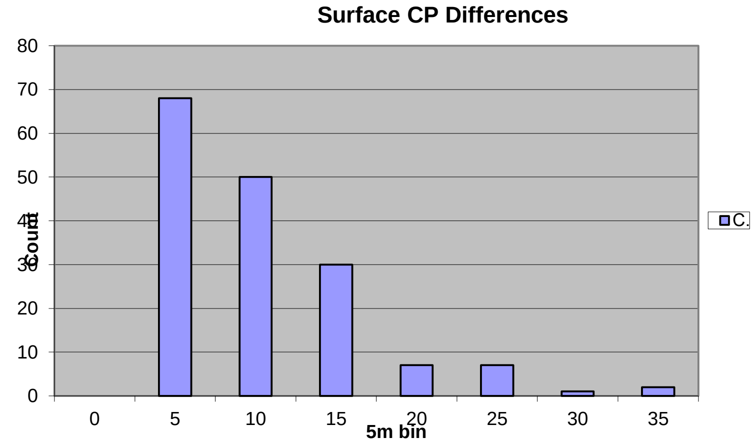

Figure 13 Surface Cross Point Difference Distribution

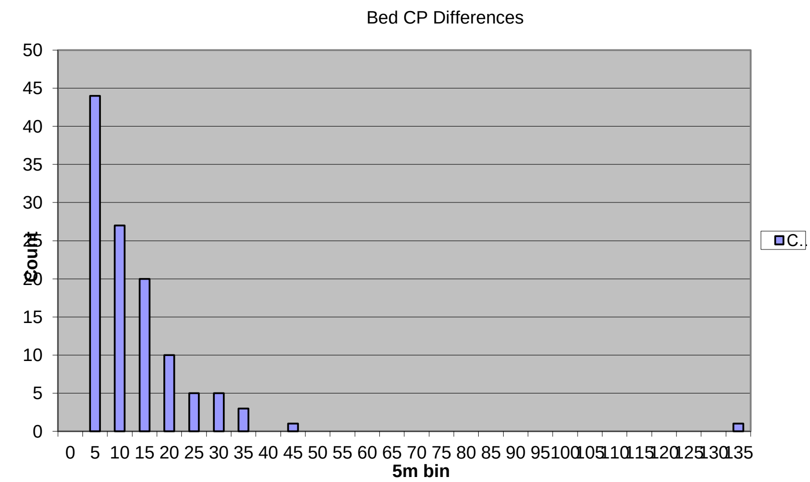

Figure 14 Bed Cross Point Difference Distribution

Scott Polar Research Institute

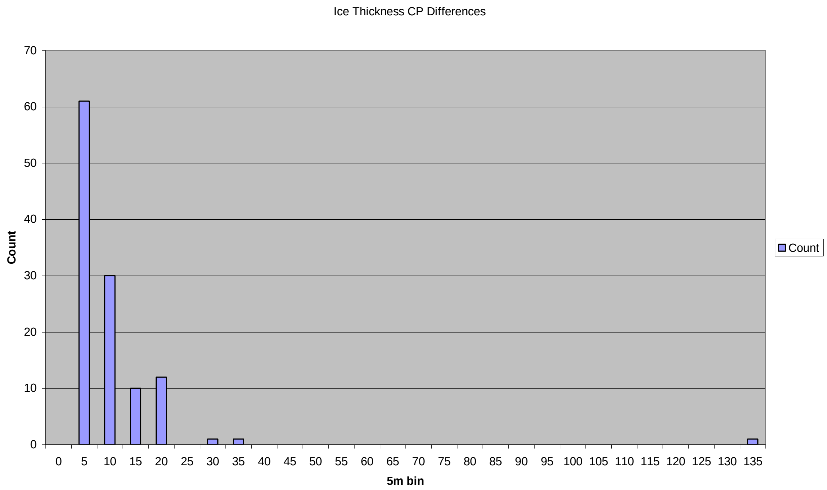

Figure 15 Ice Thickness Cross Point Difference Distribution

From these statistics, there is a good general agreement for the majority of crossover points. The points displaying the worst agreement were further investigated and found to coincide with more complicated topography. Some component of the differences observed may be due to errors in horizontal or vertical navigation data or errors and uncertainties in horizon interface tracking, although remaining irreconcilable differences may be due to the 'figure-of-eight' characteristics of the sensor footprint in relation to flight direction.

We performed some experimentation with surface horizon migration. The basic assumption, often made in analysis of RES data, is that first-return reflections come mainly from the sub-aircraft point. In fact, first returns may come from closer reflecting points along- or off-track. Migration seeks to assign reflectors to their true locations based upon the relationship of tracked points observed in consecutive waveform records. Full (3D) migration requires a high density of data lines in orthogonal directions (Welch et al., 1998). Harrison (1970) reported that a profile computed by migration of tracked points may differ significantly in form from the non-migrated profile. Our 2D (i.e. along-track) migration experimentation yielded mixed results without overall improvement. Given the overall adequacy of crossing point agreement and the resolution sought for derived DEM products, we did not pursue horizon migration further.

Error Sources

For this Level 1B product, errors in power may be due to transmitter or receiver malfunctions. Elevated background noise may occur with areas of strong surface scattering (for example crevasses) or Radio Frequency (RF) noise from anthropogenic sources (for example radio calls from the aircraft or other radar systems).

Sensor or Instrument Description

The SPRI 100 MHz radar is a VHF ice-penetrating radar which operates at a frequency of 100 MHz, with a pulse repetition frequency of 10 kHz. The system uses two half-wave dipole antennas, one mounted at a quarter-wave (0.75 m) under each aircraft wing, providing approximately 8 dB (one-way) of antenna gain. The radar is as used for earlier RES survey flying in Severnaya Zemlya, Russian Arctic, in 1997.

Michael Gorman developed the radar, building on earlier RES radar work at SPRI. This included collaboration with the Technical University of Denmark in 1975 for the joint NSF-SPRI-TUD (Scott Polar Research Institute - Technical University of Denmark) aero-geophysics program (Drewry et al., 1978; Skou and Søndergaard, 1976). Michael Gorman updated the radar for the Canadian Arctic survey.

Processing Method

During acquisition, waveform sampling is software-initiated at ~20 ms intervals. After the CompuScope CS220 AD converter detects the next transmit pulse triggered by the radar, it samples the voltage levels (as 8-bit integer values) recorded by the radar receiver over the next 256 microseconds into 'bins' of 50 ns duration, which are then retrieved by acquisition software and stored. No stacking of waveforms is performed by the radar or acquisition software.

References and Related Publications

Benham, T. J. and Dowdeswell, J. A., 2003. A simple visualization method for distinguishing subglacial-bed and side-wall returns in radio-echo records from outlet and valley glaciers. *Journal of Glaciology*, 49, 463-468.

Burgess, D. O., Sharp, M. J., Mair, D. W. F., Dowdeswell, J. A. and Benham, T. J., 2005. Flow dynamics and iceberg calving rates of Devon Ice Cap, Nunavut, Canada. *Journal of Glaciology*, 51, 219-230.

Dowdeswell, J. A. and Evans, S. 2004. Investigations of the form and flow of ice sheets and glaciers using radio-echo sounding. *Reports on Progress in Physics,* 67,1821-1861.

Dowdeswell, J. A., Benham, T. J., Gorman, M. R., Burgess, D. and Sharp, M. J., 2004. Form and flow of the Devon Island Ice Cap, Canadian Arctic. *Journal of Geophysical Research – Earth Surface*, 109(F2). doi:10.1029/2003JF000095.

Drewry, D. J. and D. T. Meldrum, 1978. Antarctic airborne radio echo sounding, 1977–78. *Polar Record,* 19, 267–273. doi:10.1017/S0032247400018271.

Mair, D., Burgess, D., Sharp, M., Dowdeswell, J. A., Benham, T., Marshall, S. and Cawkwell, F., 2009. Mass balance of the Prince of Wales Icefield, Ellesmere Island, Nunavut, Canada. *Journal of Geophysical Research – Earth Surface*, 114, doi:10.1029/2008JF001082.

Skou, N. and Søndergaard, F, 1976. Radioglaciology: A 60 MHz ice sounder system. *Technical Report R169*, Technical University of Denmark.

Van Wychen, W., Burgess, D. O., Gray, L., Copland, L., Sharp, M., Dowdeswell, J. A. and Benham, T. J., 2014. Glacier velocities and dynamic ice discharge from the Queen Elizabeth Islands, Nunavut, Canada. *Geophysical Research Letters*, 41, 484-490. doi:10.1002/2013GL058558

Williamson, S., Sharp, M., Dowdeswell, J.A. and Benham, T., 2008. Iceberg calving rates from northern Ellesmere Island ice caps, Canadian Arctic, 1999-2003. *Journal of Glaciology*, 54, 391-400.

Contacts and Acknowledgments

Prof. Julian Dowdeswell (jd16@cam.ac.uk)
Scott Polar Research Institute
University of Cambridge
Lensfield Road
Cambridge CB2 1ER
UK

Acknowledgments:

Funding: The collection of these data was funded by NERC grant GR3/12469 to J.A. Dowdeswell, as well as by grants from the Meteorological Service of Canada (CRYSYS program) to M.J. Sharp. Further funding (to J.A. Dowdeswell) for development of the dataset was provided by the NERC Centre for Polar Observation and Modelling, UK, and the EU SPICE Project.

We thank Kenn Borek Aviation for air support and the Polar Continental Shelf Project (PCSP), Canada, for ground support at Resolute Bay, and at Eureka Weather Station. We are grateful to Dr R. M. Koerner, who provided advice and support throughout the project. Prof. Liz Morris kindly assisted with data and support for GPS differential postprocessing. Waleed Abdalati, Douglas Mair and Liz Morris provided surface elevation points.

Document Information

DOCUMENT CREATION DATE:

February 2021

DOCUMENT REVISION DATE:

Scott Polar Research Institute